

# NATIONAL AIR INTELLIGENCE CENTER



DEVELOPMENTS IN INFRARED DETECTION AND TRACKING  
TECHNOLOGY AND APPLICATIONS TO MISSILES

by

He Liping

**DTIC QUALITY INSPECTED**



**Approved for public release:  
distribution unlimited**

**19960409 005**

NAIC- ID(RS)T-0633-95

**HUMAN TRANSLATION**

NAIC-ID(RS)T-0633-95      21 March 1996

MICROFICHE NR: 96000258

DEVELOPMENTS IN INFRARED DETECTION AND TRACKING  
TECHNOLOGY AND APPLICATIONS TO MISSILES

By: He Liping

English pages: 45

Source: Unknown

Country of origin: China

Translated by: Leo Kanner Associates  
F33657-88-D-2188

Requester: NAIC/TASC/Richard A. Peden, Jr.

Approved for public release: distribution unlimited.

THIS TRANSLATION IS A RENDITION OF THE ORIGINAL  
FOREIGN TEXT WITHOUT ANY ANALYTICAL OR EDITO-  
RIAL COMMENT STATEMENTS OR THEORIES ADVOC-  
ATED OR IMPLIED ARE THOSE OF THE SOURCE AND  
DO NOT NECESSARILY REFLECT THE POSITION OR  
OPINION OF THE NATIONAL AIR INTELLIGENCE CENTER.

**PREPARED BY:**

TRANSLATION SERVICES  
NATIONAL AIR INTELLIGENCE CENTER  
WPAFB, OHIO

NAIC- ID(RS)T-0633-95

Date 21 March 1996

GRAPHICS DISCLAIMER

All figures, graphics, tables, equations, etc. merged into this translation were extracted from the best quality copy available.

## DEVELOPMENTS IN INFRARED DETECTION AND TRACKING TECHNOLOGY AND APPLICATIONS TO MISSILES

He Liping

Institute No. 208, Second Academy,  
China Aerospace Industry General Corporation

**ABSTRACT:** The article generally describes the functions, work modes, cooling methods and major performance indicators of infrared detectors. Detailed presentations are given on development of infrared detection tracking technology, in addition to several infrared detectors with development prospects in weapon systems. Moreover, applications of this technology are enumerated in the field of tactical missiles, SDI project, and in the Gulf War. Finally, several proposals are made on future developments.

**Key Words:** infrared detector, infrared sensor, infrared guidance, detection.

### I. General Description

Infrared technology is extensively applied in industry, agriculture, medical treatment, sanitation, and everyday life; however, the principal applications of this technology are in military practice. In the fifties, development of PbS detectors was successful, used in the first-generation infrared guidance weapon system, such as Redeye, and the SA-7. In the mid-sixties, InSb detectors matured in technology, with applications of large

numbers of this detector type in weapon systems. This weapon is a second-generation infrared guidance weapon, such as Stinger missiles. After the mid-seventies, detectors of the HgCdTe infrared array and focal-plane infrared array types emerged as the third-generation infrared imaging guidance weapons. Rapid development of long-range infrared shows extensive prospects of infrared technology in missile guidance, as well as applications to detection and tracking [1].

The functions of the infrared sensor include conversion of infrared radiation energy of an object to electrical energy, or other easily detected forms of energy. In the infrared systems of guidance and detection tracking, the infrared sensor is the heart of such devices, and also the lodestar for development of infrared technology [2].

A complete infrared sensor includes an infrared detector and peripherals, such as preamplifier, cooler, optical system, rectifier cover, and electronic circuitry.

There are mainly three atmospheric windows of infrared radiation wavebands in military applications: 1 to 3, 3 to 5, and 8 to 12 $\mu$ m, as shown in Fig. 1 [3]. At present, the last two windows are the wavebands predominantly used in devices; in particular the last window receives the emphasis in development.

Based on work modes, infrared detectors can be divided into photoconductive detectors and photovoltaic detectors. After a semiconductor material absorbs incident photons, photoconductively generated characters are formed, changing the electroconductivity of the material through the photoconductive effect. Optical detectors based on this effect are called photoconductive detectors, as shown in Fig. 2. When a semiconductor material with space charge layer absorbs incident light at a certain energy, photoconductively generated

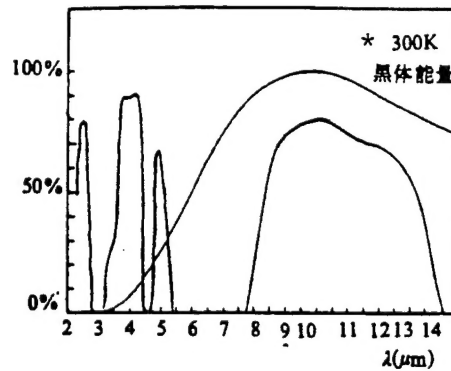


Fig. 1. Atmospheric windows sensitive to infrared  
KEY: \* - black-body energy

characters are formed. Due to carrier diffusion and the function of the electric field of the PbN junctions (space charge layer), an photoconductive electric potential is formed in the the PN junction region, generating the photovoltaic effect. When this effect is used in making a detector, it is called a photovoltaic detector, as shown in Fig. 3.

The microcooler is an indispensable component of infrared technology because an infrared detector should maintain sensitivity and frequently operates at very low temperatures. For example, when an HgCdTe detector operates between 3 and 5 $\mu\text{m}$ , the cooling is 193K (-80 $^{\circ}\text{C}$ ); when operating between 8 and 12 $\mu\text{m}$ , cooling should be 80K (-193 $^{\circ}\text{C}$ ). There should be even lower temperatures for silicon-doped and platinum silicide detectors. Fig. 4 shows three cooling methods used in infrared detectors.

## II. Major Performance Parameters of Infrared Detectors [3]

Major performance indicators include response rate, terminal wavelength, detection rate, and time constant, among others.

(1) Response rate: when an incident signal power is applied

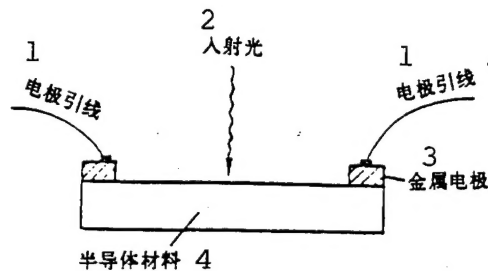


Fig. 2. Photoconductive detector

KEY: 1 - lead wire to electrode

2 - incident light 3 - metal electrode

4 - semiconductor material

normally to a sensitive surface, the mean-square-root value of the fundamental frequency voltage at the electrical output (open circuit) or the mean-square-root value of the fundamental frequency current (short circuit) with the mean-square root value of the incident radiation power is the response rate. Fig. 5 shows the ideal response rate of a detector.

(2) Terminal wavelength: this is the radiated wavelength corresponding to 50% of the maximum response rate in the related optical spectrum response curve.

(3) Detection rate: this is the ratio between the response rate when the detector sensitive surface is  $1\text{cm}^2$  and the noise equivalent bandwidth is  $1\text{Hz}$ , and the mean-square-root noise voltage or current. That is,

(4) Time constant: this is the time period during which the photocurrent is at the maximum value after the photosensitive surface is illuminated with light. Generally, this is the time

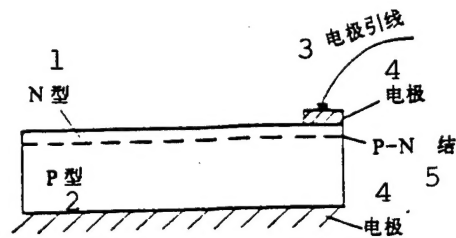


Fig. 3. Photovoltaic detector  
 KEY: 1 - N-type 2 - P-type  
 3 - lead wire to electrode  
 4 - electrode 5 - PN junction

period when the current attains 63% of its maximum value. The smaller the parameter the better it is.

Tables 1, 2, and 3 list typical infrared detectors made in China and abroad, with the principal performance indicators for typical multielement infrared detection [4]. These data represent the principal technical level attained at present. Most detectors approach the background limit infrared property (BLIP).

Worthy of note is how to properly select and rationally use infrared detectors in the infrared system, which is the key to adequately exploit the performance of infrared devices. Since the various performance parameters of infrared detectors are interrelated, overall consideration should be made during selection.

The optical spectral detection rate, temperature properties, and the relationship between the field of view of infrared detectors are shown in Fig. 6 [5], and Figs. 7 and 8. This is an important factor when properly selecting appropriate detectors. When satisfying the conditions of performance requirements of



infrared systems, one should select, if possible, infrared

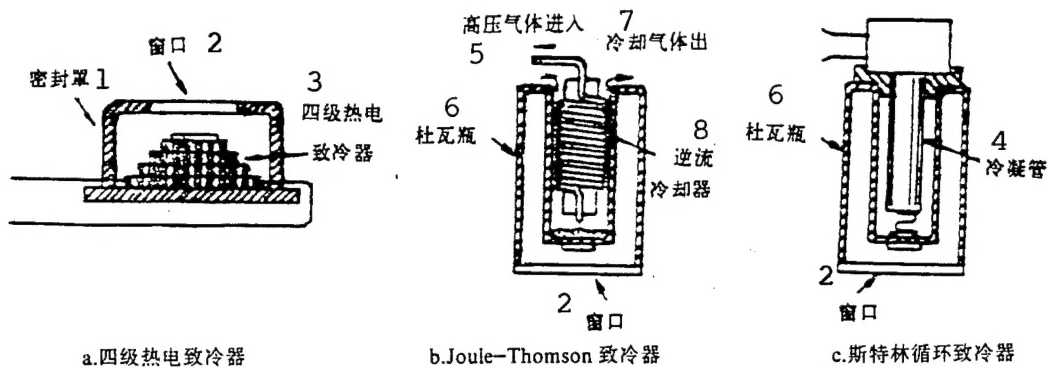


Fig. 4. Three cooling methods for infrared detectors  
a. four-level thermoelectric cooler    b. Joule-Thomson cooler    c. Stirling cycle cooler  
KEY: 1 - sealed cover    2 - window    3 - four-level thermoelectric cooler    4 - cooling and condensation tube    5 - high-pressure gas inlet    6 - Dewar flask    7 - cooling gas outlet    8 - reverse-flow cooler

detectors that have high working temperature, design simplicity, high photosensitive area, high response rate, convenience in use, and low cost.

### III. Progress in Infrared Detection and Tracking Technology [6-14]

Infrared detectors are the heart of a military infrared system. Such detectors have a unique system of high system sensitivity, good spatial resolving power, high dynamic range, high resistance to jamming, capability of 24-h round-the-clock operation in poor weather, and high capability of penetrating smoke and dust with long-wave infrared rays. Such detectors have the capability of automatic discrimination and discrimination of homing point of the target with missile-borne microcomputers [6].

Therefore, such capabilities are important for infrared imaging guidance, and detection and tracking of targets by missiles.

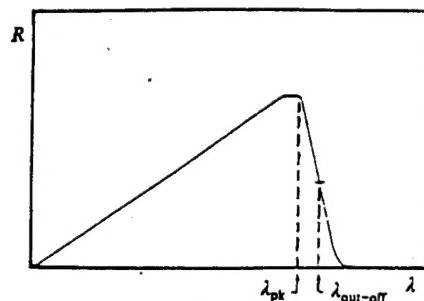


Fig. 5. Ideal response rate of detector

# 1. Progress in infrared detectors

In recent years, development of infrared detector technology has been fast-paced, from single-element, multielement, and array types to grow into the staring focal-plane array. Based on different scanning forms of infrared detectors, a presentation is made in the following text on the photo-device scanning system (line-array) and electronic scanning system (focal-plane array).

## (1) Photo device scanning system (line-array)

Thus far, mostly the line-array scanning configuration is applied in imaging infrared (IIR) sensors. A scanning optical system is applied to scan a scene and object with part of the energy focussed sequentially on every detection element. Fig. 9 shows the development of the scanning approach.

Since the seventies, rapid development took place in line-array devices made of HgCdTe material, having met the requirements for military indicators and also commercialization.



the long bands. With an applied electric field, the photocarriers are driven to move with the scanning of the light spots. When the scanning speed of the light spots is equal to

TABLE 1. Typical Performance of Foreign Infrared Detectors

1	2	3	4	5	6	7	8	9	10	11
探测器	工作方式	光敏面积( $\text{cm}^2$ )	光谱范围( $\mu\text{m}$ )	峰值波长( $\mu\text{m}$ )	响应率( $\text{V} \cdot \text{W}^{-1}$ )	探测率 $D^*$ ( $\text{cmHz}^{1/2} \cdot \text{W}^{-1}$ )	调制频率(Hz)	工作温度(K)	阻抗( $\Omega$ )	上升时间( $\mu\text{s}$ )
PbS	PC	$6.25 \times 10^{-4} \sim 1.0$	0.5~3.0	2.5	$8 \times 10^4$	$> 5 \times 10^{10}$	750	300	(0.5~15)M	<250
PbS	PC	$1 \times 10^{-2}$	0.5~2.8	2.2		$9 \times 10^{10}$	1000	300	0.5M	350
PbS	PC	$0.25 \times 10^{-2} \sim 0.16$	0.7~3.5	2.6	$5 \times 10^6$	$3 \times 10^{11}$	100	196	(0.5~50)M	~500
PbS	PC	$0.25 \times 10^{-2} \sim 0.16$	0.1~4.0	3.2	$5 \times 10^6$	$1.2 \times 11$	100	77	(1.5~50)M	
PbSe	PC	<0.16	1.0~5.1	4.4		$7.5 \times 10^9$	1000	300	2M	25
PbSe	PC		0.5~5.7	4.7	$10^6$	$2.0 \times 10^{10}$	1000	193	<20M	25
PbSe	PC	$0.25 \times 10^{-2} \sim 0.16$	0.8~7.5	5.5	$10^4$	$7 \times 10^9$	1000	77	~40M	60
InAs	PV	0.5	1.0~3.5	3.3	$6 \times 10^3$	$7 \times 10^{10}$	900	195	3000	1
InAs	PV	$10^{-2}$	1~3.2	3.1	$5 \times 10^3$	$4 \times 10^{11}$	900	77	1M	1
InSb	PC	$(1 \sim 4) \times 10^{-2}$	~7.5	6~6.3	0.4~6	$(1 \sim 8.5) \times 10^9$	800	300	30~130	0.1
InSb	PV	$10^3$	1.0~5.5	5.0	$10^3$	$1 \times 10^{11}$	900	77	1M	0.2
InSb	PV	$6 \times 10^{-6} \sim 0.25$	0.7~5.6	5.0	$2.8(\text{AW}^{-1})$	$1.1 \times 10^{11}$	1000	~145	$10^4 \sim 10^6$	0.16
InSb	PV		~5.7	5.3	$2(\text{AW}^{-1})$	~ $10^{11}$	1000	77	$10^8$	<1.0
HgCdTe	PC	$0.01 \times 0.01$	3~5	4.6		$> 1 \times 10^9$	1000	300	~100	0.4
HgCdTe	PC	$6 \times 10^{-4} \sim 0.25$	0.4~10		$10^2 \sim 10^3$	$> 2 \times 10^9$	10,000	300~77	>10	<1
HgCdTe	PC	$0.025 \times 0.02$	3~8	~5		$(1 \sim 5) \times 10^{10}$	10K	215~77	50~1K	2
HgCdTe	PC	$6 \times 10^{-5} \sim 0.25$	0.4~20	12	$10^8 \sim 10^2$	$7.2 \times 10^{10}$	10K	77	10~100	<0.5
HgCdTe	PC	$5 \times 10^{-5}$	3~12.5	11		$3 \times 10^{10}$	1000	77	50	0.25
HgCdTe	PC	$0.025 \times 0.025$	8~14	~10		$2 \times 10^{10}$	1K~10K	77	10~50	
HgCdTe	PC	$6.5 \times 10^{-6} \sim 0.1$		12		$> 2 \times 10^{10}$	2000	80	50	0.5
HgCdTe	PC	$6.5 \times 10^{-6}$		12		$> 1.5 \times 10^{10}$	10K	77	100	0.05
HgCdTe	PV	$0.015 \times 0.025$		10.6		$(1 \sim 10) \times 10^9$	带宽 200MHz	77	500	
HgCdTe	PV	$4 \times 10^{-5}$	8~14	10.6		$3 \times 10^{10}$	1800	77	>1000	$10^{-3}$
HgCdTe	PV	$10^{-4}$	8~14			$> 3 \times 10^{10}$	1800	77	>3000	
PbSnTe	PV	$0.008 \sim 3 \times 10^2$		10	$(1.5 \times 4)$ $\text{A} \cdot \text{W}^{-1}$	$(1.5 \sim 3) \times 10^{10}$		77		1~2
PbSnTe	PV	$(0.05 \sim 1) \times 10^{-2}$	5.5~12	9~11	$6 \text{A} \cdot \text{W}^{-1}$	$5 \times 10^{10}$		77		0.01
PbSnTe	PV	$0.8 \times 10^{-2}$	8~13	11	$3 \text{A} \cdot \text{W}^{-1}$	$2 \times 10^{10}$		77		0.5
Ge: Au	PC	0.034	2~11	5.0	$10^3$	$6 \times 10^9$	900	77	100K	0.5
Ge: Au	PC	$4 \times 10^{-2}$	1~9			$6 \times 10^9$	900	77	0.25M	0.1
Ge: Au	PC	$0.05^2 \times 0.3^2$	<11	5.0		$3 \times 10^9$		77	(0.5~1)M	<0.05
Ge: Hg	PC	$10^{-4} \sim 10^{-1}$	2~14	11		$3 \times 10^{10}$	1000	30	$10^4$	0.01~1
Ge: Hg	PC	$0.05^2 \sim 0.3^2$	~14	10.6		$1.7 \times 10^{10}$		5~27	0.5M	$5 \times 10^{-3}$
Ge: Hg	PC	$3.14 \times 10^{-2}$	2~15	10~11	$10^4$	$> 1.5 \times 10^{10}$	900	25	0.2M	0.05
Ge: Cd	PC	$10^{-4} \sim 10^{-1}$	5~23	22		$3 \times 10^{10}$	1000	20	$10^4$	0.01~1
Ge: Cd	PC		5~23	22		$3 \times 10^{10}$	10,000	20		
Ge: Cu	PC		~24	18		$2 \times 10^{10}$	1800	5	0.5M	
Si: Bi	PC	$10^{-4} \sim 10^{-1}$	4~17	16		~ $10^{10}$	1000	20	$10^3$	
Si: Ga	PC	$10^{-4} \sim 10^{-1}$	4~17	15		$2 \times 10^{10}$	1000	18	$10^3$	
Si: Al	PC	$10^{-4} \sim 10^{-1}$	4~18	17		$2 \times 10^{10}$	1000	20	$10^3$	
Si: As	PC	$10^{-4} \sim 10^{-1}$	6~25	23		$2 \times 10^{10}$	1000	12	$10^3$	
Si: Sb	PC		6~33	28		~ $10^{10}$	1000	4	$10^3$	

[KEY on next page]

KEY: 1 - detector    2 - operating mode    3 - photosensitive  
area    4 - optical spectral interval    5 - peak value  
wavelength    6 - response rate    7 - detection rate  
8 - modulation frequency    9 - working temperature  
10 - impedance    11 - rise time

the velocity of the carriers, the carriers generated by light at every point in an element accumulated under the influence of the electric field. Finally, the carriers accumulate at the end of the element between two electrodes, thus changing the resistive surface there with the input as the signal. This detector is also called the scanning cumulative detector. Table 4 shows its principal performance indicators.

A HgCdTe long slender band conductor with only three lead wires can obtain a performance corresponding to about 12 line-array devices. Such devices considerably simplify the electronic circuitry, thus bringing benefits to the system, dimensions, costs, and reliability. At present, there are two, four, and eight bands for the SPRITE detector, corresponding to a line-array device with 50 to 100 elements. However, its manufacturing technique is still under development. For the purpose of further improving the temperature and spatial resolving power of the imaging system.

## (2) Electronic scanning system (focal-plane array).

Although the SPRITE detector does not have electronic circuitry, yet the detector has many advantages, since it is still of a type of mechanical scanning type. An ideal detector should have the detection elements array into a rectangular array. Acting like the human eye, the pre-lens focuses the entire scene within the detector field of view on this array. Each detection element stares at a small part of the field of

view in order to absorb as much as possible of the target infrared energy. The emergence of the charge coupled device

TABLE 2. Performance Indicators of Chinese-made Infrared Detectors

探测器名称 1	工作方式 2	受光面积(mm <sup>2</sup> ) 3	视场角(°) 4	光谱范围 5(μm)	峰值波长 6(μm)	响应率 7(V·W <sup>-1</sup> )	探测率 D <sub>0</sub> <sup>max</sup> (cm <sup>2</sup> ·Hz <sup>1/2</sup> ·W <sup>-1</sup> ) 8	调制频率 9(Hz)	工作温度 (K) 10	阻抗(Ω) 11	响应时间 (μs) 12	结构特点 13
PbS	PC	0.4×0.7		1.8~3.2	>2.1	(4~9)×10 <sup>-4</sup>	(0.5~2)×10 <sup>9</sup>	400	室温	(0.3~1.5)M	100~250	石英盖板 14
PbS	PC	6×6		1.8~3.2	>2.1	(0.8~1)×10 <sup>-4</sup>	(0.5~2)×10 <sup>9</sup>	400	室温	(0.1~3)M	100~300	锗平面窗口 15
PbS	PC	0.1×0.1~6×6		0.5~3	2.1~2.4	10 <sup>-4</sup> ~10 <sup>-5</sup>	(2~8)×10 <sup>9</sup>	800	300	(0.1~2)M	100~300	晶体管外壳 16
PbS	PC	0.1×0.1~6×6		0.5~3.5	2.7~2.8	10 <sup>-4</sup> ~10 <sup>-5</sup>	(1~3)×10 <sup>9</sup>	800	193	(0.5~20)M	1000~5000	配玻璃杜瓦瓶 17
PbS	PC	0.1×0.1~6×6		0.6~4	3.1~3.4	10 <sup>-4</sup> ~10 <sup>-5</sup>	(2~4)×10 <sup>9</sup>	800	77	(0.5~20)M	1000~5000	配玻璃杜瓦瓶 18 17
PbS	PC	1.7×1.7		1~3	2.3	60~200	(3~9)×10 <sup>9</sup>	800	300	40~400K	50~150	
PbS	PC	1×1		1.8~3	2.5~2.7	>5×10 <sup>-4</sup>	(1~2)×10 <sup>9</sup>	800	293	(0.1~1)M	180~250	Φ2.5Ge 浸透透镜 18
PbS	PC	1×1		1~3	2.6	>7×10 <sup>-4</sup>	(2~4)×10 <sup>9</sup>	800	233	(0.2~1)M	200~400	硅双球面透镜 Φ6 二级 19
PbS	PC	1×1		1.8~3.2	>2.2	(1~2)×10 <sup>-4</sup>	(2~4)×10 <sup>9</sup>	800	室温	150~500K	100~300	温差电制冷 20
PbS	PC	1.6×1.6		1.8~3.2	>2.1	(2~3.5)×10 <sup>-4</sup>	(5~8)×10 <sup>9</sup>	400	29 室温	(0.1~1.5)M	100~300	锗浸透透镜 γ=1.95mm 21
PbS	PC	1.6×1.6		1.8~3.2	>2.1	(4~7)×10 <sup>-4</sup>	(4~10)×10 <sup>9</sup>	400	300	(0.3~1)M	100~300	锗浸透透镜 γ=3.8 21
PbS	PC	(1~10)×10 <sup>-4</sup>		1.6~3	2.5~2.8	10 <sup>-4</sup>	>2×10 <sup>9</sup>	800	300	(0.1~3)M		锗浸透透镜 γ=5.012 21
PbS	PC	1×1		1.6~3.2	2.4	>1×10 <sup>-4</sup>	(2~3)×10 <sup>9</sup>	800	29 室温	200~500	<318	带浸透透镜 21
PbSe	PC	1×1		1~4.8	4.4	>2×10 <sup>-4</sup>	(0.5~1)×10 <sup>9</sup>	800	233	(0.1~1)M	<16	带浸透透镜 22
PbSe	PC	1×1		1~5.2	4.8	>8×10 <sup>-4</sup>	(2~4)×10 <sup>9</sup>	800	193	(0.2~5)M	<30	硅双球面透镜 Φ6、二级 23
HgCdTe	PC	0.25×0.25	180	3~5	4.2	>1×10 <sup>-4</sup>	>5×10 <sup>9</sup>	1000	300	100~300	~1	差电制冷 24
HgCdTe	PC	0.25×0.25	180	3~5	4.6	>10 <sup>-4</sup>	(0.5~5)×10 <sup>9</sup>	1000	240	300~800	~1	二级温差电制冷 24
InSb	PV	0.1×0.1~4×4			5.3	1×10 <sup>-4</sup>	D <sub>0</sub> <sup>1</sup> = 1.2×10 <sup>11</sup>	800	77	5×10 <sup>3</sup> ~10 <sup>4</sup>	<1	
InSb	PV	Φ0.5~Φ6.2	60	3~5.5	5.0	(1~5)A/W	(0.5~3)×10 <sup>10</sup>	680	77	10 <sup>3</sup> ~10 <sup>4</sup>	<1	玻璃杜瓦瓶带金属屏蔽壳 27
InSb	PV	Φ0.5~Φ6	60	1~5.5	5.0	10 <sup>-4</sup> ~10 <sup>-5</sup>	(0.5~2)×10 <sup>10</sup>	1000	77	10 <sup>3</sup> ~10 <sup>4</sup>	<1	玻璃杜瓦瓶带金属屏蔽壳 27
InSb	PV	Φ1~Φ4.5		3~5	5±0.1	10 <sup>-4</sup> ~10 <sup>-5</sup>	D <sub>0</sub> <sup>1</sup> = (0.5~1)×10 <sup>11</sup>	1250	77	(1~30)K	<1	Φ16、Φ20 玻璃杜瓦瓶 28
HgCdTe	PC	0.2×0.2		8~14	~10		(0.5~1.5)×10 <sup>10</sup>	1000	77	30~300		玻璃杜瓦瓶带金属外壳 27
HgCdTe	PC	0.2×0.2~0.4×0.4		8~14	10.5~14	(0.5~5)×10 <sup>-4</sup>	D <sub>0</sub> <sup>1</sup> = (3~4)×10 <sup>10</sup>	2500	77	20~100		
HgCdTe	PC	0.2×0.2~0.4×0.4		8~14	10.5~14	10 <sup>-4</sup> ×10 <sup>-2</sup>	D <sub>0</sub> <sup>1</sup> = (0.6~1)×10 <sup>10</sup>	900	105	20~50	0.01~1	
HgCdTe	PV	Φ0.1~Φ0.5		8~14	11	10 <sup>-4</sup> ×10 <sup>-4</sup>	D <sub>0</sub> <sup>1</sup> = (3~4)×10 <sup>10</sup>	900	77	20~200	10 <sup>-3</sup>	
HgCdTe	PV	0.25×0.25		8~14	9~11	10 <sup>-4</sup>	D <sub>0</sub> <sup>1</sup> = (2~3)×10 <sup>10</sup>	1250	77	30~200	<0.1	玻璃杜瓦瓶 28
HgCdTe	PV	(5~20)×10 <sup>-2</sup>	60	8~14	10~12	(1~6)AW <sup>-1</sup>	D <sub>0</sub> <sup>1</sup> = (1~4)×10 <sup>10</sup>	630	77	50~1000	0.2~0.02	玻璃杜瓦瓶 28
HgCdTe	PV	0.5×0.5	180	8~14	~10		D <sub>0</sub> <sup>1</sup> = (0.8~2.4)×10 <sup>10</sup>	1000	77	50~1000	<0.01	金属杜瓦瓶 28
PbSnTe	PV	Φ0.1~Φ0.5	60	8~14		>10 <sup>-4</sup>	D <sub>0</sub> <sup>1</sup> = (1~3)×10 <sup>10</sup>	1000	77	>30	0.2	
PbSnTe	PV	0.3×0.3~0.6×0.6		8~14	11.7		D <sub>0</sub> <sup>1</sup> = 2.3×10 <sup>10</sup>	900	77	500~1000	0.1	
Ge:Hg	PC	0.5×0.5		8~14	10.6	5×10 <sup>-4</sup>	~10 <sup>10</sup>	800	30	(50~100)k	<0.01	

[KEY on next page]

KEY: 1 - name of detector    2 - operating mode    3 - area  
receiving light    4 - angle of field of view    5 - optical  
spectral interval    6 - peak value wavelength    7 - response rate  
8 - detection rate    9 - modulation frequency    10 - working  
temperature    11 - impedance    12 - response time  
13 - structural features    14 - quartz cover plate  
15 - germanium flat window    16 - transistor    17 - fitted with  
Dewar glass flask    18 - immersion lens    19 - OD6 silicon dual-  
surface spherical lens, two levels    20 - thermocoupling electric  
cooling    21 - germanium immersion lens    22 - band immersion  
lens    23 - silicon dual-surface spherical lens    24 - two levels  
of thermocoupling electric cooling    25 - four-level  
thermocoupling electric cooling    26 - conditions of germanium  
immersion    27 - Dewar glass flask with metal shield in shell  
28 - Dewar glass flask

(CCD) opened a route for the above-mentioned requirements, by installing the CCD onto an integrated module of the detector array. The CCD stores and processes the signal detected by the sensor. Without scanning, on seeing an object through a reflecting mirror the entire field scene can be observed in the same time period. The higher the number of detection elements, the higher is the sensitivity of the system, and the higher is the resolving power of the possible image output [8].

With respect to infrared imaging guidance of a focal-plane array, it improves the thermal sensitivity so that the detecting distance is extended and the discrimination rate is enhanced. With numerical processing by using an appropriate algorithm with thermal data from the array, the target signal can be provided and the target with the highest threat level can be determined. By designing a more effective optical system and adopting the advanced circuitry packaging, the size of the device can be reduced in order to reduce power consumption.

At present, the focal-plane array structure under development is divided into single-chip type or hybrid type. In the single-chip type, the detector and the CCD are fabricated on

the same semiconductor material. They are unable to reach optimization together; frequently, optimization at one layer

TABLE 3. Performance Indicators of Typical Multielement Infrared Detectors

探测器名称 <sup>1</sup>	波长范围 <sup>2</sup> ( $\mu\text{m}$ )	工作方式 <sup>3</sup>	探测率 $D^*$ ( $\text{cm} \cdot \text{Hz}^{1/2} \cdot \text{W}^{-1}$ ) 19	上升时间 <sup>5</sup> ( $\mu\text{s}$ )	元件尺寸 <sup>6</sup> ( $\mu\text{m}^2$ )	元件间隔 <sup>7</sup> ( $\mu\text{m}$ )	8 元件数目 13	9 制备方法	工作 温度 10 (K)	备注 <sup>11</sup>
PbS	1~3	PC	平均 $2 \times 10^{10}$		25 × 25	15	1024(多达 2000)	化学淀积 <sup>12</sup>	171	
PbSe	3~5	PC	(2~4) × $10^{10}$		25 × 500	50	64(多达 140) <sup>13</sup>	化学淀积 <sup>12</sup>	193	
InSb (平面膜版) <sup>18</sup>	3~5	PV	$D_{500\text{K}}^* > 2 \times 10^{10}$		250 × 250	50	34(多达 556) <sup>13</sup>	离子注入 $\text{Zn}^{14}$	77	
InSb	3~5	PV	19	16	40 × 40	20	140		77	28
HgCdTe	3~5	PC	平均 $D^*$ (500k, 20k Hz, 1) $0.9 \times 10^{10}$	最大 0.4	50 × 50	12.5	10~64		195	四级温差电制冷
HgCdTe	8~14	PC	平均 $D^*$ (500k, 20k Hz, 1) $2 \times 10^{10}$	最大 3	50 × 50	12.5	48		77	
HgCdTe	8~14	PC	平均 $D^*$ (500k, 20k Hz, 1) $2 \times 10^{10}$	最大 0.4	50 × 50	12.5 或 18 <sup>15</sup>	50		> 65	36° 视场 <sup>29</sup>
HgCdTe	8~14	PC	$D^*$ (500k, 20k Hz, 1) $0.9 \times 10^{10}$	0.3	50 × 50	12.5	195(100~200)		77	60° 视场 <sup>29</sup>
HgCdTe	2~12.5	PC	$4 \times 10^{10}$	0.4			20		77	$\lambda_p = 11\mu\text{m}$ , $R_v = 1.5 \times 10^2 \text{V} \cdot \text{W}^{-1}$
HgCdTe	8~14	PC			40 × 40	8	180		77	
HgCdTe	8~14	PC	$D^*$ (10.5 $\mu\text{m}$ , 5k Hz, 1) $2 \times 10^{10}$		50 × 50	25	10	扩散 <sup>21</sup>	77	180° 视场 <sup>29</sup>
HgCdTe	8~14	PV	$D^*$ (10 $\mu\text{m}$ , 1k Hz, 1) $6 \times 10^{10}$		100 × 100	25	80		77	30° 视场 <sup>29</sup>
HgCdTe	8~14	PV	$\text{NEP} = 6 \times 10^{-20} \text{W} \cdot \text{Hz}^{-1}$	20			4		77	4MHz 四象限外差, $\lambda_p = 1.06\mu\text{m}$ , 60° <sup>30</sup> 视场, 最小 $\text{NEP} < 1 \cdot 10^{19} \text{W} \cdot \text{Hz}^{-1}$ <sup>31</sup>
HgCdTe	8~14	PV	$D^*$ (10.5 $\mu\text{m}$ ) $1 \times 10^{11}$				20~200 <sup>14</sup>	外延 离子注入 <sup>22</sup>	77	截止 / > 1000MHz <sup>31</sup>
PbSnTe	8~14	PV	$2 \times 10^{10}$		150 × 250	250	43 <sup>23</sup>	异质液相外延 <sup>24</sup>	77	$R_o \text{Ad} 2\Omega \cdot \text{cm}^{-2}$ <sup>29</sup>
PbSnTe / PbTe	8~14	PV	$2.3 \times 10^{10}$		$6 \times 10^{-3} \text{mm}^2$		18	液相外延	80	2 $\pi$ 视场, 300K 背景 <sup>32</sup>
In-PbSnTe <sup>17</sup>	8~14	PV	$3.5 \times 10^{10}$		$7.33 \times 10^{-3} \text{mm}^2$		25 <sup>25</sup>	分子束外延	77	$\lambda_p = 10\mu\text{m}$ , 180° 视场
肖特基势垒			$2.2 \times 10^{10}$ (9.8 $\mu\text{m}$ )							
P-PbSnTe /	8~14	PV	$1 \times 10^{11}$ (4.6 $\mu\text{m}$ )				12(各 6) <sup>26</sup>		80	
P-PbTe	3~5									
Ge,Hg	8~14	PC			100 × 100	50	60(多达 180) <sup>27</sup>		35	

[KEY on next page]



KEY: 1 - name of detector    2 - wavelength interval  
 3 - operating type    4 - detection rate    5 - rise time  
 6 - dimensions of element    7 - spacing of elements  
 8 - number of elements    9 - preparatory method  
 10 - working temperature    11 - remarks    12 - chemical  
 deposition    13 - as many as    14 - ion implantation  
 15 - or    16 - maximum    17 - Schottky potential barrier  
 18 - flat fitted    19 - average    20 - frequency response  
 21 - diffusion    22 - epitaxial    23 - heterogeneous liquid-  
 phase epitaxy    24 - liquid-phase epitaxy    25 - molecular-  
 beam epitaxy    26 - (six each)    27 - as many as    28 - four  
 levels of thermocoupling electric cooling    29 - field of  
 view    30 - four-quadrant epitaxy    31 - field of view,  
 minimum    32 - background

leads to reduced performance at another layer. In the hybrid type, the detector array and the CCD layer can reach optimization separately. Then interconnections are made. In the present status, the hybrid structure is more emphasized than the single-chip structure with faster development. Generally, hybrid integration is made with photovoltaic detectors and Si-CCD. Fig. 10 [9] shows a typical structure of the hybrid type infrared CCD with a combination of photovoltaic HgCdTe detector and a Si-CCD.

Under development is another method of realizing the focal-plane array; this is the Z-technique [10, 11]. Several ceramic chips with lead wire patterns overlapping each other involve internal circuits in the ceramic chip. The input signal of the sensor is sent by a lead wire according to the specified routing to the analog signal processor, and multichannel transmitter integrated circuit, installed on the ceramic chip. Then the sensor is installed on the edge of the ceramic chip layers. This structure provides wide-open prospects for advanced signal processing. If the silicon integrated circuit replaces the ceramic chip, the design can be more compact; the output of each row of detection elements is directly coupled onto the input terminal of the silicon chip. The position of the silicon chip is vertical to the detection element chip (in the Z-plane). This

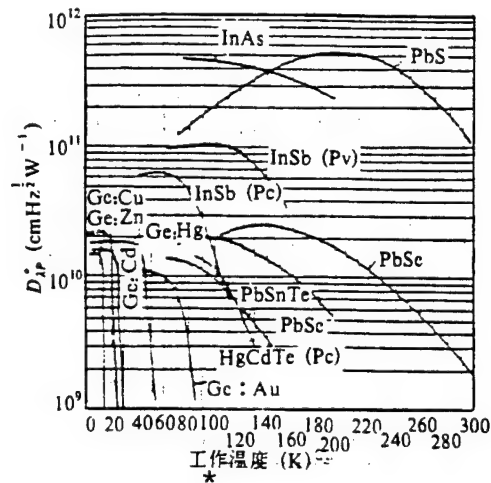


Fig. 7. Detection-temperature property of typical infrared detectors  
KEY: \* - working temperature

chip can process a signal, and also cancel out jamming. The output of the processor chip is fed to the second level processor, whose position is face to face and parallel with the array chip (on the XY-plane). Thus, very high densities can be realized by keeping the processor physically closer to the detection element. However, costs under this method are very high.

To enable a focal-plane array to be applied to missiles and other systems in large lots, cutting production costs is very important. Increasing the end product yield and reducing the substrate dimensions are the key to lower costs. In the Pave Pace project in the United States, the main target is to reduce the production costs of the focal plane array from 60,000U.S. dollars for each focal-plane array at present, to less than 1,000U.S. dollars.

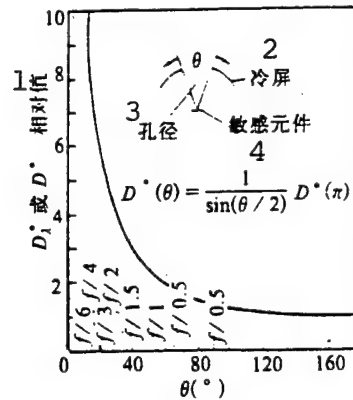


Fig. 8. Relation between detection rate and field-of-view angle of infrared detectors  
KEY: 1 - relative value 2 - cooled shield  
3 - aperture 4 - sensitive element

has attempted to comprehensively apply the silicon substrate manufacturing technique, as well as the experience and production equipment in order to mass produce low-cost focal-plane arrays. Fig. 11 shows the production process. By adopting the interconnection method as shown in Fig. 12, of the vertical integrated metal insulated semiconductor (VIMIS) to interconnect the infrared detector and the integrated circuit processor, by keeping good contacts.

In another production method, as adopted by the Rockwell Corporation in the upgrading project of Pace I, the focal-plane array production line with sapphire substrate. In the production process, the HgCdTe grown with extension at a low temperature adheres to the substrate so as to realize high uniformity and stable sensitivity. In addition, through indium contact pads, each detection element is directly connected with the silicon integrated chip, as shown in Fig. 12. It was stated that the

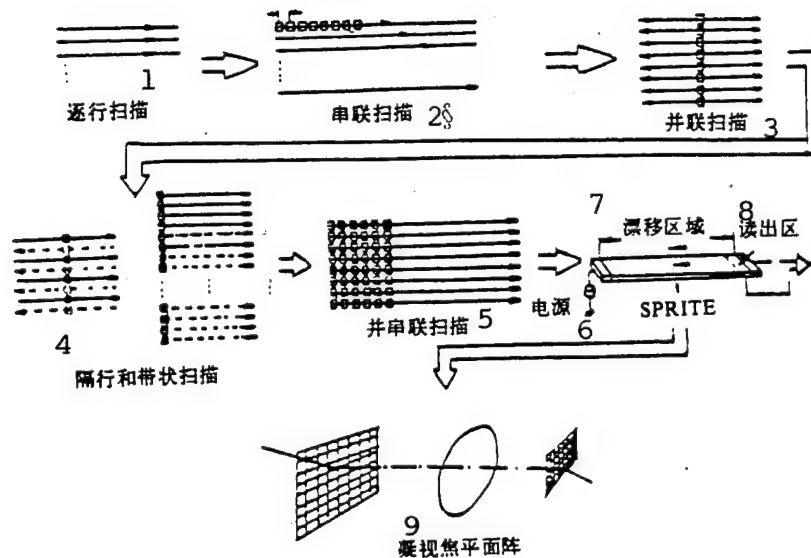


Fig. 9. Schematic diagram of single-element scanning of staring-type focal-plane array development  
 KEY: 1 - line-by-line scanning 2 - serial scanning  
 3 - parallel scanning 4 - scanning at alternate lines and zone scanning 5 - parallel and serial scanning 6 - power supply 7 -drift region  
 8 - readout zone 9 - staring-type focal-plane array

density is the highest with this packaging, along with good interconnections and without shielding against incident thermal radiation.

TABLE 4. Main Properties of SPRITE Detector

材 料 17	n-HgCdTe	n-HgCdTe
探测元数量 1	8	8
条形片子长度( $\mu\text{m}$ ) 2	700	700
光敏面(瞬时)( $\mu\text{m}^2$ ) 3	$62.5 \times 62.5$	$62.5 \times 62.5$
工作波长( $\mu\text{m}$ ) 4	8~14	3~5
工作温度(K) 5	77	190
致冷方式 6	节流或热机 15	温差电 16
偏置场强( $\text{V} \cdot \text{cm}^{-1}$ ) 7	30	30
迁移率( $\text{cm}^2 \cdot \text{V}^{-1} \cdot \text{s}^{-1}$ ) 8	390	140
像元速率(像元 $\cdot \text{s}^{-1}$ ) 9	$1.8 \times 10^6$	$7 \times 10^5$
探测元典型阻值( $\Omega$ ) 10	500	$4.5 \times 10^3$
每探测元功耗(mW) 11	9	1
探测器总功耗(mW) 12	<80	<10
平均 $D^*$ (500K, 20kHz 1, $62.5 \times 62.5 \mu\text{m}^2$ )( $\text{cm} \cdot \text{Hz}^{1/2} \cdot \text{W}^{-1}$ ) 13	$> 11 \times 10^{10}$	$(4 \sim 7) \times 10^{10}$
响应率 $R$ (500K, $62.5 \times 62.5 \mu\text{m}^2$ ) $\times (\text{V} \cdot \text{W}^{-1})$ 14	$6 \times 10^4$	

KEY: 1 - number of detection elements 2 - length of strip-shaped foil 3 - photosensitive surface (instantaneous)  
 4 - working wavelength 5 - working temperature 6 - cooling method 7 - bias field intensity 8 - transfer rate 9 - speed of picture element (picture element  $\cdot \text{s}^{-1}$ ) 10 - typical resistance of detection element 11 - power consumption for each detection element 12 - total power consumption of detector  
 13 - average 14 - response rate 15 - throttling or heat engine 16 - thermocoupling electricity

In the Pace I stage, up to now the largest hybrid focal-

plane array that can be produced is the 256x256 40 $\mu$ m-element detector. It is estimated that if a 5.08cm substrate is used, calculated on the basis of a 0.5% yield rate at present, daily

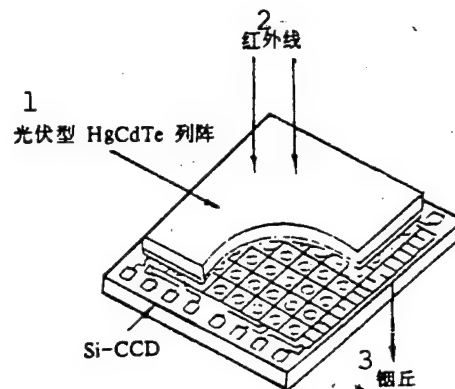


Fig. 10. Hybrid type infrared CCD structure  
KEY: 1 - photovoltaic type HgCdTe array  
2 - infrared array 3 - indium pad

output should be 5000substrates in order to satisfy the annual demand of half a billion picture elements in the nineties, corresponding to 9U.S. dollars per picture element. The goal of the Defense Strategic and Tactical Reproduction (DSTAR) of the Defense Advanced Research Project Agency in the United States is to use 7.2cm substrates for a yield rate of up to 15%, and the cost of each picture element to be lowered to 5cents. Thus, the daily output of nearly 50substrates can satisfy the above-mentioned goal. Generally, with respect to infrared focal-plane arrays, manufacturing costs and technology are always problems of concern to the parties involved.

## 2. Development of infrared signal processing [12, 13]

In the nineties, with development of tracking reconnaissance toward real-time capability, infrared sensors used for detection and tracking will have very high data rates. Therefore, this

requires adopting high-speed hardware with parallel processing, with adoption of computer graphic signal processing, including preprocessing (graphics enhancement and division) video signal

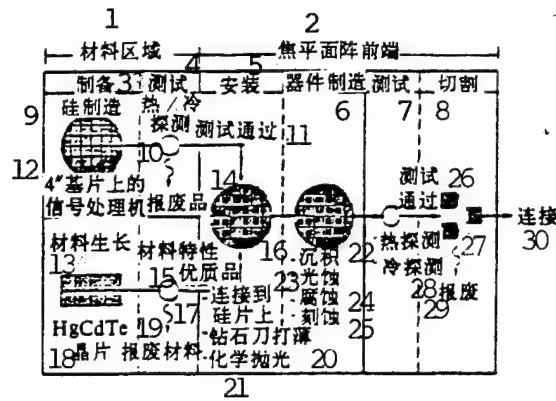


Fig. 11. Focal-plane array fabrication flow chart at TI Corporation

KEY: 1 - region of material 2 - front end of focal-plane array 3 - preparation  
 4 - measurement and testing 5 - mounting  
 6 - fabrication of device 7 - measurement and testing 8 - cutting 9 - silicon fabrication  
 10 - hot/cold detection 11 - passed measurement tests 12 - signal processor on 4-inch substrate  
 13 - growth of material 14 - reject product  
 15 - material properties 16 - high-grade product  
 17 - interconnections to silicon chip 18 - chip  
 19 - reject material 20 - thinning with diamond cutter 21 - chemical polishing  
 22 - sedimentation 23 - optical etching  
 24 - corrosion etching 25 - carved etching  
 26 - passed measurement and testing 27 - hot detection 28 - cold detection 29 - reject  
 30 - interconnections

frequency processing (target feature extraction and classification of decision-making), and target position data processing (to have control command). As required by preprocessing, the computational rate is  $5 \times 10^6$  operations per second. Development of very-high-speed integrated circuits

(VHSIC) provides the possibility of computations at high density and superhigh speeds. It is estimated that by the end of the century, the silicon integrated circuit will have matured in

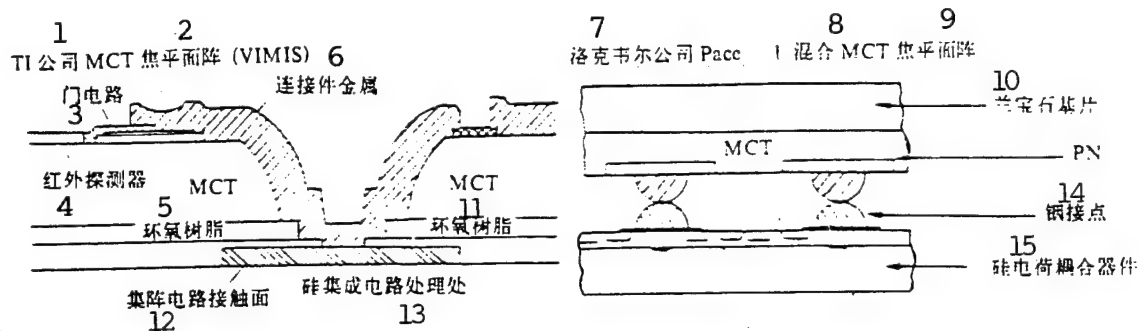


Fig. 12. Schematic diagram of focal-plane array interconnections  
 KEY: 1 - TI Corporation 2 - focal-plane array  
 3 - gate circuit 4 - infrared detector  
 5 - epoxy resin 6 - connector metal  
 7 - Rockwell Corporation 8 - mixed  
 9 - focal-plane array 10 - sapphire substrate  
 11 - epoxy resin 12 - contact surface of  
 integrated-array circuit 13 - processing site  
 of silicon integrated circuit 14 - indium  
 contact pad 15 - silicon charge-coupled device

technology; the number of transistors contained on each piece of integrated circuitry will be tens of millions, even up to 100million, 100times the present number of transistors.

With respect to the infrared focal-plane array sensors, adoption of advanced graphic signal processing technique is the key to achieving intelligent sensors [10]. Further development of the signal processing technique, including the matching of each detection element on the focal-plane array, uniform response on about 1% of the terminal wavelengths, with compensation attained from optical filtering and signal processing.



Development of VHSIC will further promote upgrading of the information processing technique. With the development of the advanced infrared focal-plane array of very high density and very

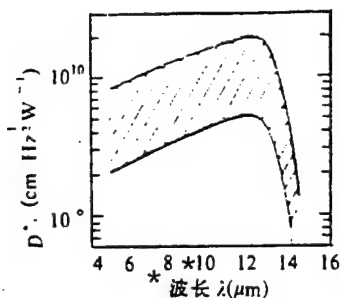


Fig. 13. Optical spectral detection rate of HgCdTe detector  
(working temperature: 77K, 10° to 130°, field of view, 300K background, photosensitive area  $4 \times 10^{-5}$  to  $4 \times 10^{-2} \text{cm}^2$ )  
KEY: \* - wavelength

high picture element number, one can determine the upgrading of the parallel techniques. For example, the SIMD (single-instruction/multiple data) configuration already used in focal-plane arrays, this parallel technique will move toward superhigh-performance and highly compilation simplification. In addition, with the development toward parallel-coupling with the local number of processing elements and a large number of high-speed data memories, this will provide more conventional computational capability for real-time processors of focal-plane graphics.

### 3. Superconducting infrared focal-plane array of the future [14]

The development of superconducting technology makes the application possible on space-based brand-new sensor technology

based on superconductivity. The advantages of using the superconducting circuits of low-heat dissipation used in focal-plane arrays are as follows: heating is no more the principal restraining factor in chip-making of high processing capability.

TABLE 5. Major Performance Indicators of HgCdTe Detectors

参数名称 1	光电导型 2	光伏型 3
工作温度(K) 4	77	77
时间常数( $\mu$ s) 5	$\sim 1$	$< 0.1$
光谱范围( $\mu$ m) 6	8~14	8~14
探测率 $D_1$ ( $\text{cm} \cdot \text{Hz}^{1/2} \cdot \text{W}^{-1}$ ) 7	$> 1 \times 10^{10}$	$> 1 \times 10^{10}$

KEY: 1 - name of parameter    2 - photoconductive type  
 3 - photovoltaic type    4 - working temperature  
 5 - time constant    6 - optical spectral interval  
 7 - detection rate

It is very easy to carry out analog-to-digital conversion by using superconducting circuitry. Digital processing related to target motion can be handled with chips. All such digital output can be mixed into a single electro-optical modulator, to modulate the fiber optic light beam and to communicate with the outside world. It is estimated that the power consumption in accomplishing the above-mentioned functions is only a fraction of the semiconductor focal-plane array at present. Moreover, it is possible to utilize the available superconducting manufacturing technique to make large focal-plane arrays of several square inches. This will be revolutionary progress with respect to the technology of infrared focal-plane arrays.

#### IV. Several Types of Infrared Detectors with Development Prospects [15-20]

To explain the development of infrared detection and tracking technology to the next step, below we present HgCdTe, platinum silicide and bichromatic detectors with

TABLE 6. Performance Indicators of Bichromatic Detectors

测试条件 1		
黑体温度 2	500K	
背景温度 3	300K	
元件温度 4	77K	
辐射通量密度 5	$2\mu\text{W} / \text{cm}^2$	
带 宽 6	6Hz	
窗口材料 7	IRTRAN-2	
探测器间隔 8	0.005"	
结果 9	PbSnTe	InSb
探测器面积( $\text{cm}^2$ ) 10	0.02	0.045
开路电压(mV) 11	11	98
短路电流( $\mu\text{A}$ ) 12	6	2.2
零偏压阻抗( $\text{k}\Omega$ ) 13	3.2	530
零偏压电容(pF) 14	940	32
峰值响应率( $\times 10^5 \text{V} / \text{W}$ ) 15	0.046	6.25
$D^*(500,900,1)(\times 10^{10} \text{cm} \cdot \text{Hz}^{1/2} / \text{W})$	0.41	1.7
$D^*(\lambda_p,900,1)(\times 10^{10} \text{cm} \cdot \text{Hz}^{1/2} / \text{W})$	1.45	8.5

KEY: 1 - measurement and test conditions 2 - blackbody temperature 3 - background temperature 4 - element temperature 5 - density of radiation flux 6 - bandwidth 7 - window material 8 - detector spacing 9 - results 10 - detector area 11 - open-circuit voltage 12 - short-circuit current 13 - impedance at zero bias 14 - capacitance at zero bias 15 - peak value response rate

development prospects in miliary applications.

### 1. HgCdTe infrared detectors

Because of the physical properties of HgCdTe material, this

is the best material from which to make infrared detectors, with the most applications in the 8 to 12 $\mu$ m waveband. Table 5 and Fig. 13 show its principal performance indicators and parameters.

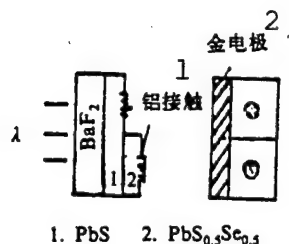


Fig. 14. Structure of bichromatic detector  
KEY: 1 - aluminum contact pad    2 - gold electrode

The advantages of HgCdTe are as follows [15]: (1) the material can be used for infrared detection in various response wavebands; (2) high response rate; (3) large photoelectric gain factor; (4) high quantum efficiency; and (5) high sensitivity. However, there are disadvantages to HgCdTe: cooling is necessary; homogeneity of picture elements is not sufficiently ideal; and higher production costs. After many years' research, the HgCdTe material fabrication technique has grown in maturity, with the properties of crystal, structure, and physical performance being fairly well understood. Not only have good-performance single-element and line-array detectors been fabricated, but HgCdTe is also the most important material in developing focal-plane arrays. The most 128x128 intermediate wave HgCdTe array made by Rockwell Corporation has a quantum efficiency of 64%; by using 60 $\mu$ m-diameter picture elements, helicopters as far away as 8km have been detected. At night time, nonoperating armored vehicles 4.5km away can be detected.

## 2. Platinum silicide infrared detectors [16]

Among the more materials that are more sensitive to infrared radiation, besides HgCdTe with the most applications in the focal-plane array, another very attractive material for stare-

TABLE 7. Performance Indicators, Application Status and Key Techniques of Some Foreign Infrared Imaging Guided Missiles

国别 1	型 号 2	性能指标 3	应用现状 4	关键技术 5
美国 6	"幼畜" 10 AGM-65D	20 电视、红外成像、激光三种 导引头, 对付地面各种目标	32 1974 年研制, 1983 年具有 作战能力, 1993 年大批装备	多元红外成像技术图像处 理, 小型光机扫描系统 43
	"拉姆" 11 RAM	雷达与红外双模被动导引头, 对付反舰导弹 21	1979 年研制, 1980 年试飞, 拟于 1986 年后装备 33	被动雷达导引头与被动红 外天线通用复合 44
	"海尔法" 12 AGM-114A	激光半主动, 红外成像和射 频—红外三种导引头对付装 甲目标 22	1972 年研制, 1982 年投产, 1984 年大批装备 34	激光指示和通用导弹控制 系统 45
	"黄蜂" 13 Wasp	毫米波雷达与红外成像制 导, 攻击机动装甲 23	1982 年研制, 1986 年生 产, 1988 年装备 35	识别技术, 数据处理, 天 线罩 46
	"战斧" 14 BGM-109A	红外成像制导, 巡航高度 1.2km 24	1972 年研制, 1982 年生产, 1988 年装备 36	图像处理, 大规模集成计 算机 47
	"坦克破坏者" 15	凝视焦平面成像, 攻击坦克、 直升机 25	1981 年研制, 1982 年试验, 尚未装备 37	凝视焦平面成像技术 48
	"先进巡航导弹" 16	红外、毫米波制导 26		
跨国 7	"ADATS" 防 空、"反坦克导弹" 17	雷达、电视、光学、红外成 像及激光制导对付飞机、装 甲、坦克 27	1979 年研制, 1981 年试 验, 1984 年后装备 38	两用精度协调, 两用战斗 部协调 49
苏联 8	SA-9	被动红外成像制导 28	已装备 39	
美国 6	"中程空空导弹" (AMRAAM) 18	凝视焦平面 4096 元和 1024 × 1024 元制导 29	40 1983 年论证, 90 年代装备 41	多元探测, 多路信息传 输、处理和计算机 50
英国 9	"近程空空导弹" (ASRAAM) 19	凝视焦平面 1024 × 1024 元 制导 30	40 1983 年论证, 90 年代装备 41	多元探测、多路信息处理 和计算机 51
苏联 8	AS-13	被动红外成像制导 31	在研制中 42	

[KEY on next page

KEY: 1 - nation 2 - model number 3 - performance indicator  
4 - application status 5 - techniques 6 - United States  
7 - multinational category 8 - Soviet Union 9 - United  
Kingdom 10 - Bullpup 11 - RAM 12 - Hellfire 13 - Wasp  
14 - Tomahawk 15 - Tank destroyer 16 - Advanced cruise  
missiles 17 - air defense and antitank missiles  
18 - intermediate air-to-air missiles 19 - short-range air-to-  
air missiles 20 - three guidance heads of television, infrared  
imaging and laser to deal with various ground targets  
21 - radar and infrared dual mode passive guidance heads to deal  
with antiship missiles 22 - three kinds of guidance heads:  
laser semiactive, infrared imaging, and radio-frequency--  
infrared, to deal with armored targets 23 - millimeter radar  
and infrared imaging guidance to attack motorized armor  
24 - infrared guidance, cruise height at 1.2km 25 - staring-  
type focal-plane imaging to attack tanks and helicopters  
26 - infrared and millimeter wave guidance 27 - radar,  
television, optics, infrared imaging, and laser guidance, to deal  
with aircraft, armor, and tanks 28 - passive infrared imaging  
guidance 29 - staring-type focal-plane 4096-element, and  
1024x1024-element guidance 30 - staring-type focal plane  
1024x1024 element guidance 31 - passive infrared imaging  
guidance 32 - development in 1974, combat capability in 1983,  
and deployment in large numbers in 1993 33 - development in  
1979, test flight in 1980, scheduled to deploy after 1986  
34 - development in 1972, production in 1982, and deployment in  
large numbers in 1984 35 - development in 1982, production in  
1986, and deployment in 1988 36 - development in 1972,  
production in 1982, and deployment in 1988 37 - development in  
1982, experimentation in 1982, not yet deployed  
38 - development in 1979, experiments in 1981, and deployment  
after 1984 39 - already deployed 40 - verification in 1983,  
deployed in the nineties 41 - verification in 1983, deployed in  
the nineties 42 - in development 43 - multielement infrared  
imaging technique, graphics processing, small optical device  
scanning system 44 - passive radar guidance head, and passive  
infrared antenna applications 45 - laser indication and general  
missile control system 46 - discrimination technique, data  
processing, and antenna dome 47 - graphics processing with  
large-scale integrated computer 48 - staring-type focal-plane  
imaging technique 49 - dual-usage precision coordination and  
dual-usage warhead coordination 50 - multielement detection,  
multichannel information transmission, processing and computer  
51 - multielement detection, multichannel data processing and  
computer

type material is platinum silicide.

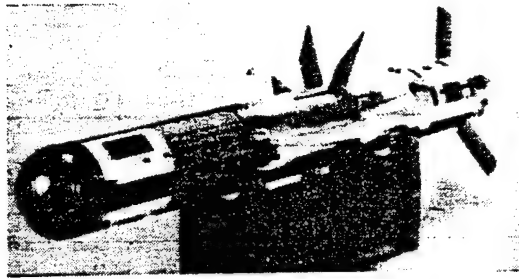


Fig. 15. AAWS-M guided missile

Platinum silicide detectors rely on photoradiation technology to detect infrared photons, which collide on the platinum electrode of the detector, stimulating electrons entering the silicon chips. Beneath the platinum silicide thin layer, the silicon integrated circuit is a detector array with multiple converters that collect signal charges from each detection element, to convert the charges into a video-frequency readout signal. This signal should be amplified with synchronizing pulses to be able to display the infrared pictures on a monitor.

In fabricating the platinum silicide detector, first the platinum is vaporized at 2000C for deposition on a silicon integrated circuit several feet away. When platinum arrives at the silicon chip, the metal vapor temperature has been reduced to hundreds of degrees centigrade. However, as mentioned above, the molten platinum silicide does not cover the entire detector surface, because there are silicon processing circuits around the rectangular platinum silicide.

Production costs are the key factor determining the success of new detector models. One of the principal reasons for

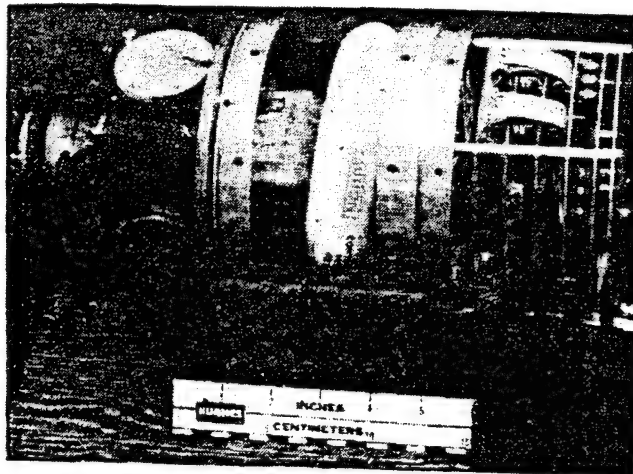


Fig. 16. FOG-M infrared guidance head

platinum silicide being highly regarded is its low costs, although its sensitivity is not as good as that of HgCdTe. By coating 3 to 5 $\mu$ m in the intermediate infrared window, the cost is considerably lower than that of HgCdTe. Every picture element with HgCdTe detection costs, in terms of dollars, while a picture element of a platinum silicide detector costs only cents. At present, some companies and research centers are developing a detector array chip containing 250,000 to 300,000 picture elements, in two specifications of 512x512, and 486x640 picture elements. The 1024x1024 elements, as an array including more than 1 million picture elements, is also expected to become available several years in the future.

The quantum efficiency of platinum silicide is not as good as HgCdTe, but its homogeneity is better. Moreover, only 16% of the picture elements covered by a platinum silicide detector should be improved; the other portions are covered by the electronic readout data circuits. Thus, the problem can be



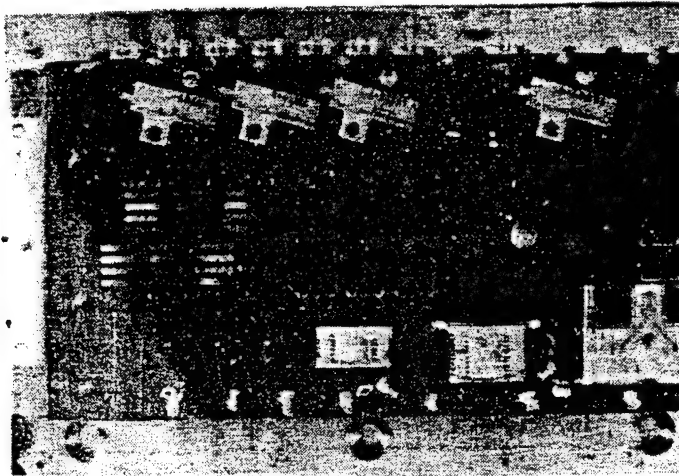


Fig. 17. There are 15 modules in focal-plane array of AOA sensor; each module has four sensor chip arrays, including 640 detection elements. One module in the picture cannot be seen

solved by fabricating a hybrid device. In other words, the detector and readout equipment are separated by two silicon chips, which are interconnected with indium contact pads with ceramic chip packaging. In this way, the interstitial coefficient at the top of the silicon chip can be as high as 95%, so that almost the entire surface of the picture elements have a detector function. The multiple conversion circuit is placed on the second block\*, thus becoming more complicated in order to process signals with very wide dynamic variation range. With shrinkage of the silicon integrated circuit and improvements in processing, at present it is possible to put the multiple converter and detector on the same piece of material, capable of simultaneously attaining high interstitial coefficient.

One property of the platinum silicide detector that is noteworthy is to separate the backgrounds between  $\text{CO}_2$  and the

infrared energy that can be radiated. This has important military value, because CO<sub>2</sub> gas is included in the exhaust of aircraft and missile engines.

### 3. Gallium arsenide detectors [17, 18]

Gallium arsenide infrared detectors are noteworthy. Together with HgCdTe, gallium arsenide has the same property of detecting long-wave infrared.

At Bell Laboratories in the United States, an entirely-new method was used in fabricating gallium arsenide infrared detectors. The entire physical detection process is also different. Gallium arsenide is used to replace HgCdTe, and a sandwich structure, which the HgCdTe detector lacks, is applied. By using silicon doping, 40Angstrom thick cavities are formed to provide a mechanism for detecting photons. Cavities are separated by the gallium aluminum arsenide potential barrier; the substrate is a piece of gallium arsenide. This new infrared detector is modulated by changing the cavity depth and constituents of the potential barrier, capable of detecting wavelengths between 6 and 10 $\mu$ m. Up to the present time, the most effective detectors that have been fabricated are used in detecting 8- $\mu$ m wavelengths. The advantage of this approach is that the high speed gallium arsenide field-effect transistor (FET) can be integrated with the infrared detector onto a single piece of material. However, the HgCdTe detector requires the use of a silicon semiconductor exclusively to fabricate circuitry. Since a single piece of gallium arsenide material can be used to fabricate electronic circuitry and detection devices, this is very useful in fabricating focal-plane array detectors. In addition, the gallium arsenide focal-plane array is possibly ten times cheaper than the HgCdTe.

Besides, integrated circuitry using gallium arsenide is five

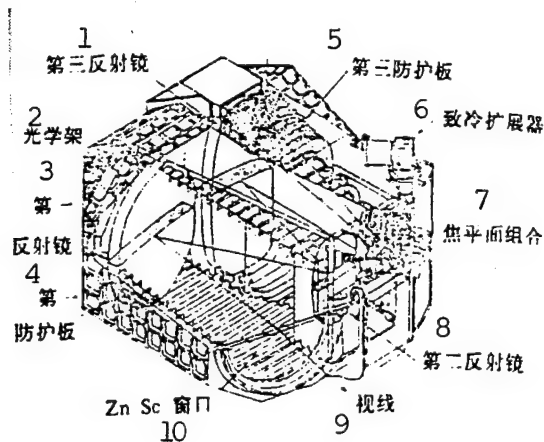


Fig. 18. Three-surface molten quartz reflecting mirror to reflect photons onto a focal-plane complex, 15 inches long, in AOA sensor. The complex has 38,400 detection elements, with low-temperature cooling.

KEY: 1 - third reflecting mirror 2 - optical frame 3 - first reflecting mirror 4 - first protective plate 5 - third protective plate 6 - cooling expander 7 - focal-plane complex 8 - second reflecting mirror 9 - line of sight 10 - ZnSc window

times faster in operating than when using silicon, with a wide adaptation range and low power consumption, so that gallium arsenide is an indispensable material for supercomputers and optical communications. Moreover, the properties of gallium arsenide are higher with respect to cosmic rays and nuclear radiation; this is an ideal material for space military applications. Infrared sensors used in ballistic missile defense (BMD) systems should have the capability of withstanding intense radiation from nuclear blasts far away. The present infrared detectors are fabricated from thicker silicon and HgCdTe

materials, since these materials are easily damaged by nuclear blasts. Gallium arsenide detectors can meet the requirements of withstanding radiation in the BMD system.

However, like HgCdTe, this new type of detector can operate only after being cooled down to 77K. Liquid nitrogen is required for cooling. There are some differences from monolithic silicon elements, in that defects easily occur internally during crystallization, thus bringing difficulties to the high integration of integrated circuitry. Further research is required to overcome this difficulty.

#### 4. Bichromatic detectors [19]

With advances in precision guidance, it appears very important to measure and compare two or more wavebands in the infrared spectrum. The so-called bichromatic or multichromatic detector involves using two or more responses in different wavebands to make a sandwich structure type detector, capable of simultaneously detecting radiation from two or more wavebands. After the seventies, bichromatic detectors, such as InSb/HgCdTe (1 to 5 $\mu$ m)/5 to 15 $\mu$ m), and the InSb/PbSbTe (1 to 5 $\mu$ m/5 to 12 $\mu$ m), were developed in the United States with mature preparatory techniques. Table 6 shows the principal performance indicators.

Fig. 14 shows a new bichromatic detector structure developed for the U.S. Navy. The unique features are intense display signals and good discrimination. The key technical process is to use vacuum vaporization to grow a 5 $\mu$ m-thick epitaxial p-type PbS layer 5 $\mu$ m on a transparent BaF<sub>2</sub> substrate, then a stainless steel foil cover plate is deposited over half the Pb layer with a 5 $\mu$ m-thick epitaxial layer of PbS<sub>0.5</sub>Se<sub>0.5</sub>P. On two epitaxial layers line-array a circular-shaped Pb electrode is vaporized, thus fabricating a bichromatic photovoltaic detector. The goal in

this research is to obtain, finally, a multichromatic focal-plane detector.

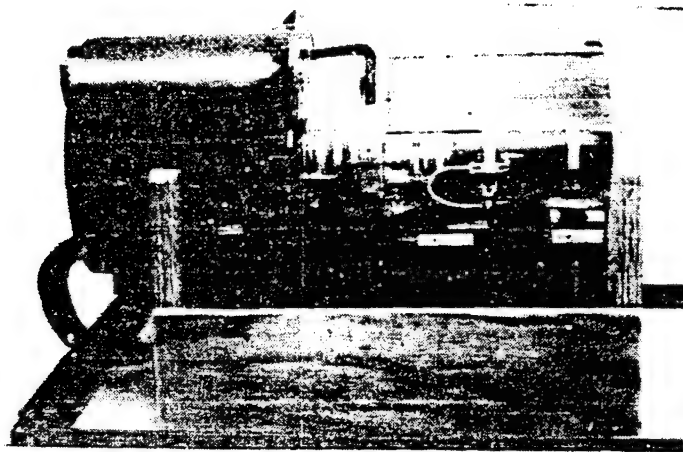


Fig. 19. Built by Martin-Marrieta Corporation, guidance head used for SBI, including high-speed imaging processor and focal-plane array bichromatic sensor

## V. Applications of Infrared Detection and Tracking Technique [20-32]

### 1. Applications in tactical missiles

Infrared detectors are widely used in weapon guidance; up to now, infrared guidance has been used in 60 to 70 missile models.

In combat, infrared guided missiles demonstrate precision guidance. In the past, for more than a decade more than 90% of known aircraft losses in wars were downed with infrared missiles [20]. In particular, infrared imaging guidance technology greatly upgrades weapon performance. Table 7 lists performance indicators of some infrared imaging guidance missiles made abroad, together with application status and key techniques [21]. The first finalized models of an infrared imaging missile, the Bullpup AGM-65D and AGM-65F in the United States, have been in lot production, deployed among troop units. However, missile improvements are still continuing. At the Hughes Corporation, development is underway on computer artificial intelligence and expert systems of graphic processing techniques by extracting information from graphics. In other words, a large-capacity memory is installed in a missile to store detailed information on the target selected, the scanning environment during missile flight, and an automatic search and retrieval database in order to upgrade missile performance.

Bichromatic guidance technique is one of the present important direction of development in precision guidance munitions. At present, more than ten type of bichromatic guidance cannon rounds and guided missiles have been developed, such as the SA-13 of the former Soviet Union, the improved Stinger version of the United States, and the TAN-SAM made in Japan. Bichromatic guidance utilizes the frequency spectrum difference between a target (such as an aircraft, missile, or tank) and the background (such as sky, sea surface, and ground objects), as well as various kinds of jamming. In the case of the U.S. Stinger missile, CdS/InSb ( $0.3\mu\text{m}/3$  to  $5\mu\text{m}$ ) is employed, by using an  $0.3\mu\text{m}$  (the peak scattering density value of sunlight) ultraviolet detector to distinguish between the target and the sky background, and a 3 to  $5\mu\text{m}$  infrared detector to detect and track thermal energy radiated by aircraft (the peak value of radiation lies between 4 and  $5\mu\text{m}$ ). Development is underway, in

the United States, on a bichromatic imaging system in the 3 to 5 $\mu$ m and the 8 to 13 $\mu$ m wavebands. The goal is to develop an imaging guidance head by using a 128x128bichromatic array.

An important technique of infrared sensors in order to achieve innovation in the future progress of infrared weapons is the infrared focal-plane array [10]. Beginning with recent development, the new-generation tactical missiles will apply the focal-plane array technique. For example, the portable advanced antitank weapon system--intermediate type (AAWS-M) of the U.S. Army, the fire-and-forget missile [15]) applies a 64x64 staring-type focal plane array. The thermal imaging instrument of the command launch unit (CLU) applies a 241x1scanning focal plane array for a wide field of view.

Besides the application of long-wave HgCdTe scanning and staring-type arrays by the AAWS-M, the advanced missile system-heavy version (AMS-H) and the over-the-horizon air defense/antitank missile (FOG-M, also called the fiber-optical guided missile), will also apply the focal-plane imaging guidance head. What has been adopted by the AMS-H is the long-wave HgCdTe 128x128 staring-type array. However, the FOG-M will plan to adopt the intermediate platinum silicide staring-type array. Previously, a platinum silicide staring-type focal-plane array was developed at the Hughes Corporation, for the IIR guidance head (Fig. 16) of the FOG-M, with the adoption of a 256x256-structure, for a total of 56,536detection elements. Later, the company developed a larger 244x244staring-type array. Since the 114-pound FOG-M can contain more electronic equipment, the larger the array, the better the resolving power of video frequency that can be provided.

## 2. Applications in SDIO program

One of the 15 important experimental projects in the SDI program is research on long-wave infrared sensors [25].

Consideration was given to installing such sensors in the Space Surveillance and Tracking System (SSTS) satellite to detect reentry ICBM nose cones. Developed under the SDI program, the long-wave infrared sensors have successfully tracked the targets launched from the Vandenburg Air Force Base. The present long-wave infrared detection technology has the capability of detecting, from 1000 nautical miles away in cold outer space, a target with heat emitted by a human body. The long-wave infrared detection technique can be used not only to detect and track terminal reentry nose cones, but also can detect and track targets in the unpowered flight stage above the atmosphere, in order to gain precious early warning time for terminal defense. In the SDI program, nearly 1000 early warning satellites primarily adopt the long-wave focal-plane array. In development at the present, the dynamic energy interceptor missile will also adopt the infrared detection and automatic tracking technique. It can be seen that the infrared focal-plane detection and tracking techniques have important standing in the SDI program [24].

#### (1) Satellite-borne infrared sensors [23]

Infrared sensors carried by infrared early warning satellites can detect missiles in the boost-phase. The maximum sensitivity is concentrated in the  $0.3\mu\text{m}$  wave window. By using the 3 to  $5\mu\text{m}$  intermediate wave window, although the energy liberated by the booster rocket is less than  $1.5\mu\text{m}$  at  $3.5\mu\text{m}$ , yet the absolute energy is large; therefore, within tens of seconds (50s, in the case of the United States) after launch of a strategic missile, the satellite-borne sensor can detect with 30min of early warning time for antimissile defense. Since 1971, satellite-borne infrared sensors of the United States have detected more than 1000 launches of ballistic missiles by the Soviet Union, China, and France.

#### (2) Aircraft-borne infrared sensors



There is good detection capability of aircraft-borne infrared sensors used in detecting ballistic missiles. The U-2 high-altitude reconnaissance craft carried infrared heat sensors for the emergency early warning system. The infrared telescope has a field of view  $-2$  to  $20^\circ$ , wavelength between  $8$  and  $12\mu\text{m}$ , aperture  $20.3\text{cm}$ , and focal length  $91.4\text{cm}$ , capable of seeing targets in the upper atmospheric layers. To enhance the aircraft-borne early warning capability, the Air Force made improvement in stages in order to have  $125,000$  array elements, and an action distance as far as  $4775$  nautical miles, capable of detecting various ICBM models in the boost phase.

Besides, the airborne optical apparatus (AOA) under development in the United States will also be used in BMD [25]. In this case, the infrared sensor is carried on aircraft to supplement ground radar in missile defense. The focal length set for the sensor is  $15$  inches, including  $60$  detector chips, and  $640$  infrared detection elements for each array. With indium, the detector connects with a preamplifier having the same number of detection elements to amplify the signal slightly before entering the readout circuit.  $38,400$  gallium-doped silicon detection elements are installed on  $15$  modules, as shown in Figs. 17 and 18, in order to assess the performance in tracking and detecting missiles.

### (3) Infrared guidance head of interceptor

As indicated by space-based interceptor (SBI) experiments in the SDI program [26], the SBI technique can be used to intercept ballistic missiles in the boost phase. Fig. 19 shows the guidance head of the staring-type focal-plane array of SBI, capable of discovering and locking on the target. As revealed in experiments, the SBI sensors, signal processors, and software can process simultaneously large amounts of signals in order to

discriminate the very bright exhaust plume from a solid-state rocket engine from the missile proper.

Under development at present is the light extra-atmospheric projectile (LEAP) project [27] with infrared homing. The LEAP project will be used to track and intercept targets in the boost phase, as well as in the late and intermediate phases. This project also includes the infrared imaging sensor electronic equipment, inertial sensor equipment, thrust-vectoring sensor, thermocoupling battery set, and the command data link, used in the kinetic kill system. The terminal homing sensor guidance system and the thrust-vectoring engine controlled by the onboard missile computer can ensure target interception. This year's experiment will verify the performance of 16,384 elements of a 128x128 HgCdTe focal-plane array [28].

### 3. Applications in the Gulf War

In local wars in recent wars, the infrared early-warning satellites and early warning reconnaissance aircraft have been important means of detection and reconnaissance [29]. In this Gulf War, three early warning satellites were used. During limited visibility, or with camouflage colors painted on launchers leading to difficult-to-discriminate situations, the KH-12 Keyhole satellite 850km from the ground can utilize image forming and infrared scanning methods to detect heat energy from fired missiles in order to find their location. In addition, this satellite is responsible for photographing crisply clear pictures such as the serial number on the missile launcher.

Since the SCUD missile launchers of Iraq are mobile, sometimes reconnaissance satellites are not able to precisely discover their tracks. The GR1 Hurricane reconnaissance of the U.K. Royal Air Force exploited important functions [30]. At the forward undernose surface of the GR1, an infrared detection system is installed, capable of precisely detecting the tracks of

the SCUD, to inform friendly aircraft for attack. In the second round attack against Iraq, the GR1 successfully smashed six missile launchers.

TABLE 8. Optoelectronic Guided Weapons Emerging in the Gulf War

1 国别 1	名称 4	5 类别	6 制导体制
2 多国部队	BGM-109C“战斧” 7	17 巡航弹	惯导+地形匹配+红外成像末制导 22
	“幼畜”AGM-65D 8	18 空-地	红外成像制导 23
	“轻剑” 9	19 防空弹	光学/电视或雷达跟踪+无线电指令
	“幼畜”AGM-65A/B	18 空-地	电视制导 25 24
	“罗兰特 II” 10	20 地-空	光学跟踪+无线电指令 26
	“尾刺”-POST 11	20 地-空	红外、紫外双色寻的 27
	“西北风” 12	20 地-空	红外寻的 28
	“响尾蛇”AIM-9 系列 13	21 空-空	红外制导 29
	“海尔法”反坦克导弹 14	18 空-地	激光半主动 30
	GBU-15, AGM-130	18 空-地	电视制导 25
	“宝石路”, AS.30 15	18 空-地	激光制导炸弹 31
3 伊军	SA-9, SA-13 等 16	20 地-空	红外制导 29
	SA-14	20 地-空	激光驾束 32

[KEY on next page]

KEY: 1 - nation    2- multinational troops    3 - Iraqi troops  
 4 - name    5 - category    6 - guidance system    7 - Tomahawk  
 8 - Bullpup    9 - Lightsword    10 - Roland    11 - Stinger  
 12 - Northwesterly    13 - Rattler, AIM-9 series    14 - Hellfire  
 antitank missile    15 - Gemroad    16 - et al.    17 - cruise  
 missiles    18 - air-to-ground    19 - air defense missiles  
 20 - ground-to-air    21 - air-to-air    22 - inertial guidance +  
 terrain-matching + infrared imaging terminal guidance  
 23 - infrared imaging guidance    24 - optical/television or radar  
 tracking + radio command    25 - television guidance  
 26 - optical tracking + radio command    27 - infrared/ultraviolet  
 bichromatic homing    28 - infrared homing    29 - infrared  
 guidance    30 -laser semiactive    31 - laser-guided bomb  
 32 - laser-driven beam

In the Gulf War, infrared guidance missiles played an important role with gigantic intimidation power. Table 8 shows the photoelectronic guidance weapons that emerged during the Gulf War. By using the example of the Bullpup missile, in the period with the most intensive air raids, upwards of 100 Bullpup missiles were launched each day [31].

The precision guidance capability of infrared guidance weapons is relatively high, with high hit rates. Coordinated with other weapons, the infrared guidance weapon exerted its function in the war.

Variations in the modern war environment spurred the development of infrared night vision systems. To gain the initiative on the battlefield, troops should have fighting capability either day or night.

In the Gulf War, infrared night vision equipment exhibited high functions. The AH-64 Apache armed helicopter, and the UH60A Blackhawk helicopters of the United States are equipped with thermal imaging reconnaissance systems and advanced night vision devices. Although the Iraqi Soviet-made Mi-24 attack craft were also equipped with FLIR [forward-looking infrared] night vision,

their performance was poorer than those on the American craft. An advanced night vision equipment, the cat's-eye night vision instrument for pilots of the U.S. Navy and the Marine Corps, costs more than 700,000U.S. dollars per set [32]. Infrared night vision equipment is extensively used in various electronic warfare aircraft, such as the F-117, the F4G, and the F-16 fighters, as well as the EA-6B and the EF-111A of the United States Air Force, and the M-1 tanks of the U.S. Army.

## VI. Several Suggestions for Future Developments

### 1. Emphasize the development of guidance technology

The Gulf War was the largest scale high-tech war for weaponry since World War II. Precision guidance of weapons was one of the features of the war. Long-wave infrared imaging guidance technology and bichromatic guidance technology for precision guidance in the future have had further development. Research on the staring-type focal-plane array and the graphic processing will be further upgraded. As to the development directions of guidance, on the one hand, novel detection devices are under development, and, on the other hand, further research into hybrid guidance, has developed toward the hybrid guidance of integrating radar, television, lasers, and infrared multiple detection and tracking methods. With respect to tactical missiles in China, especially air defense missiles, this is also the direction that we should pursue.

### 2. Emphasize the development of infrared materials production techniques.

To apply the advanced infrared focal-plane array technique, costs should be cut, and large-lot production can be carried out. For example, large-lot production of focal-plane arrays has been the emphasis in the United States, with research of key

techniques such as materials growth, and applying chemical vapor deposition and growth techniques of metal and organic compounds for use in fabricating HgCdTe epitaxial growth layers. Moreover, photoelectric diodes will be grown on substrates of buffer gallium arsenide. Moreover, some low-cost materials (such as platinum silicide and gallium arsenide) are to be researched and produced in missile guidance heads in order to cut costs. In the case of China, the HgCdTe production technology still lags behind the developed nations to some extent. While pushing the development of advanced production technology, importation of advanced technology for production in China is also a right approach, thus speeding up the upgrading of precision guidance performance of tactical weapons in China.

3. Infrared detection and tracking requires that data processing should keep pace in its advance.

VHSIC enables the concentrated type high-speed graphics processing. In the case of China, while developing the staring-type infrared array devices, research on other related supplementary techniques should also proceed, laying a foundation for artificial intelligence in missiles.

4. Development of infrared countermeasures technology is a factor that should not be overlooked.

The emergence of precision guidance munitions will surely give rise to countermeasures. The infrared guidance system promotes the development of infrared countermeasures technology. In the Gulf War, the infrared countermeasures techniques also were quite active. Wars in the future will involve comprehensive countermeasures of multiple sensors in the sea, land, and air, in coping with communications, radar, and the command and control network. We should carry out automatic search, acquisition, analysis, and discrimination of threats from multiple targets

from all directions and in all frequency bands. In our case, while developing precision guidance munitions, infrared countermeasures technology is also a factor that cannot be overlooked. We should conduct system verification and simulation research on infrared countermeasures.

5. Development of infrared night vision equipment should be placed on the agenda.

Night war will be the principal mode in wars of the future. By using the long-wave infrared detection techniques in night vision equipment, night warfare capability can be further upgraded. Advanced infrared night vision equipment was installed in various branches of the U.S. Armed Forces. In the case of China, mass production and deployment of night vision instruments will be included in the military program to upgrade the night warfare capability of the Chinese Armed Forces.

#### References

- [1] "A Hot Issue: Infra-red Sensors and Infra-red Countermeasures", Military Technology, 9 / 1990, pp.97-105.
- [2] 《红外探测器的现状及未来趋势》，红外，1990年7月，第1-4页。
- [3] "Infra-red Detectors", Military Technology, 2 / 1989, pp.56-64.
- [4] 杨道华等编，《激光与红外技术手册》，国防工业出版社。
- [5] "A Little Warmth. A Little Light", Journal of Electronic Defense, April'90, pp.47-56.
- [6] "Toward Lower-cost Focal-plane Arrays", Interavia Aerospace Review, 11 / 1989, pp. 1123-1126.
- [7] 张秀媚、龚琰民，《红外成像制导技术的现状与前景》，航空航天部三院八三五八所。
- [8] "New Army IR-Guided Missile to Rely on Focal Plane Arrays in the 1990s", Armed Forces Journal International, May 1989, pp.72-76.
- [9] 《日本的HgCdTe红外列阵探测器》，红外，1990年9月，第8-9页。
- [10] "New Horizons for IR Focal-plane Array." Photonics Spectra, July 1988, pp.125-128.
- [11] "Senaora for SDI", Defenae Science and Electronica, May 1987, pp.36-38.
- [12] "Recent Development in Infrared Data Processing", SPIE, Volume 694, pp.150-157.

- [13] 何启予,《红外成像制导系统与发展趋势》, 航空航天部三院八三五八所。
- [14] “超导红外焦平面阵列”, Naval Research Review, three / 1989, pp.3-8.
- [15] 《红外探测器的发展概况》, 激光与红外, 1991 年 1 月, 第 5~11 页。
- [16] “Platinum Silicide Detectors Incorporated into New Generation of Missile Seekers”, Aviation Week & Space Technology, March 27, 1989, pp.51-62.
- [17] “日本的毫米波、红外和砷化镓技术”, 军事研究, 昭和 62 年 3 月 1 日, 第 96-102 页。
- [18] “Bell Labs Report Breakthrough In Gallium Arsenide IR Detectors”. Aviation Week & Space Technology. Sept. 5, 1988, p.205.
- [19] 《双色红外探测器》, 红外技术, 1989 年 8 月, 第 29~34 页。
- [20] “Infrared Countermeasure: A Point of View”, Journal of Electronic Defense, April'90, pp.41-46.
- [21] 《红外成像技术的军用现状及发展前景》, 激光与红外, 1990 年 3 月, 第 24~28 页。
- [22] “智能导弹即将问世”, Interavia, 7 / 1986, pp.747-748.
- [23] “SDI: Technology Survivability and Software”, May 1988, Chapter 4, pp.73-101.
- [24] 《红外探测器焦平面阵技术在美国SDI计划中的地位》, 华中工学院, 第三届全国光电器件科技交流会。
- [25] “Boeing Prepares AOA Sensor for Flight Test on 767”, Aviation Week & Space Technology, November 7, 1988, pp.40-41.
- [26] “SBI Tests Demonstrate Technologies Could Work on other Missile Defenses”. Aviation Week & Space Technology, Feb.26, 1990, pp.27-28.
- [27] “Infrared Homing Projectile Provide Kinetic Kill Defense”. Signal, June 1990, p.46.
- [28] “Leap Begins Flight Tests to Demonstrate Kinetic Kill Missile Defense Capability”, Aviation Week & Space Technology, June 17, 1991, p.207.
- [29] 《美卫星侦察扫描敌阵》, 新联合晚报, 1991 年 1 月 24 日。
- [30] 《英旋风战机红外线功能高》, 新联合晚报, 1991 年 1 月 24 日。
- [31] “Infrared Signatures—What Iraqi Tank Force Can't Hide”. International Herald Tribune, 1991, 2.21.
- [32] 《夜袭系统, 美国唯我独尊》, 新联合晚报, 1991 年 1 月 26 日。



DISTRIBUTION LIST

DISTRIBUTION DIRECT TO RECIPIENT

ORGANIZATION	MICROFICHE
B085 DIA/RTS-2FI	1
C509 BALLOC509 BALLISTIC RES LAB	1
C510 R&T LABS/AVEADCOM	1
C513 ARRADCOM	1
C535 AVRADCOM/TSARCOM	1
C539 TRASANA	1
Q592 FSTC	4
Q619 MSIC REDSTONE	1
Q008 NTIC	1
Q043 AFMIC-IS	1
E404 AEDC/DOF	1
E410 AFDTC/IN	1
E429 SD/IND	1
P005 DOE/ISA/DDI	1
1051 AFIT/LDE	1
PO90 NSA/CDB	1

Microfiche Nbr: FTD96C000258  
NAIC-ID(RS)T-0633-95